J|A|C|S
ARTICLES
Published on Web 10/12/2006

Direct Nitric Oxide Detection in Aqueous Solution by Copper(II) Fluorescein Complexes

Mi Hee Lim,[†] Brian A. Wong,[†] William H. Pitcock, Jr.,[‡] Deepa Mokshagundam,[†] Mu-Hyun Baik,*[,‡] and Stephen J. Lippard*[,†]

Contribution from the Department of Chemistry, Massachusetts Institute of Technology, Cambridge, Massachusetts 02139, and the Department of Chemistry and School of Informatics, Indiana University, Bloomington, Indiana 47405

Received July 13, 2006; E-mail: mbaik@indiana.edu; lippard@mit.edu

Abstract: A series of FL_n ($n = 1-5$) ligands, where FL_n is a fluorescein modified with a functionalized 8-aminoquinoline group as a copper-binding moiety, were synthesized, and the chemical and photophysical properties of the free ligands and their copper complexes were investigated. UV−visible spectroscopy revealed a 1:1 binding stoichiometry for the Cu(II) complexes of FL_1, FL_3, and FL_5 in pH 7.0 buffered aqueous solutions. The reactions of FL_2 or FL_4 with $CuCl_2$, however, appear to produce a mixture of 1:1 and 1:2 complexes, as suggested by Job's plots. These binding modes were modeled by the synthesis and X-ray crystal structure determination of Cu(II) complexes of 2-[(quinolin-8-ylamino)methyl]phenol (modL), employed as a surrogate of the FL_n ligand family. Two kinds of crystals, $[Cu(modL)_2](BF_4)_2$ and $[Cu_2(modL')_2(CH_3OH)](BF_4)_2$ (modL′ = 2-[(quinolin-8-ylamino)methyl]phenolate), were obtained. The structures suggest that one oxygen and two nitrogen atoms of the FL_n ligands most likely bind to Cu(II). Introduction of nitric oxide (NO) to pH 7.0 buffered aqueous solutions of Cu(FL_n) (1 μM $CuCl_2$ and 1 μM FL_n) at 37 °C induces an increase in fluorescence. The fluorescence response of Cu(FL_n) to NO is direct and specific, which is a significant improvement over commercially available small molecule-based probes that are capable of detecting NO only indirectly. The NO-triggered fluorescence increase of Cu(FL_5) occurs by reduction of Cu(II) to Cu(I) with concomitant dissociation of the *N*-nitrosated fluorophore ligand from copper. Spectroscopic and product analyses of the reaction of the FL_5 copper complex with NO indicated that the *N*-nitrosated fluorescein ligand (FL_5−NO) is the species responsible for fluorescence turn-on. Density functional theory (DFT) calculations of FL_5 versus FL_5−NO reveal how *N*-nitrosation of the fluorophore ligand brings about the fluorescence increase. The copper-based probes described in the present work form the basis for real-time detection of nitric oxide production in living cells.

Introduction

Nitric oxide (NO) is produced in a biological context by nitric oxide synthases.[1−6] The properties of NO allow for its varied involvement in physiological and pathophysiological pathways,[3,4,6,7] but the details of how it performs its biological roles are not fully understood. The development of a method capable of detecting NO in biology has been an intriguing challenge for chemists, biologists, and engineers. Small-molecule fluorescent sensors for NO have the potential to provide a practical method for visualizing its presence and movement in vitro and in vivo.[8,9]

A few basic requirements are necessary for the design of biologically useful fluorescent NO probes,[8,9] including water-solubility, cell-membrane permeability, and visible or near-IR excitation and emission wavelengths. Most importantly, these sensors must have the capability for direct, specific, and rapid detection of NO. In addition, sensors that give fluorescence enhancement by reaction with NO are preferred for imaging NO in biological systems over those that respond to NO with a fluorescence decrease.

The commonly used, current generation of NO probes is based on organic molecules.[8,10] Although these probes satisfy the basic requirements for bioimaging NO, they have the critical limitation that their fluorescence response is not driven by NO, but by an oxidized NO species. This requirement means that

[†] Massachusetts Institute of Technology.
[‡] Indiana University.

(1) Murad, F. *Angew. Chem., Int. Ed. Engl.* **1999**, *38*, 1856−1868.
(2) Leone, A. M.; Palmer, R. M. J.; Knowles, R. G.; Francis, P. L.; Ashton, D. S.; Moncada, S. *J. Biol. Chem.* **1991**, *266*, 23790−23795.
(3) Moncada, S.; Palmer, R. M. J.; Higgs, E. A. *Pharmacol. Rev.* **1991**, *43*, 109−142.
(4) Conner, E. M.; Grisham, M. B. *Methods Enzymol.* **1995**, *7*, 3−13.
(5) Marletta, M. A.; Hurshman, A. R.; Rusche, K. M. *Curr. Opin. Chem. Biol.* **1998**, *2*, 656−663.
(6) Ricciardolo, F. L. M.; Sterk, P. J.; Gaston, B.; Folkerts, G. *Physiol. Rev.* **2004**, *84*, 731−765.
(7) Packer, L. *Methods in Enzymology, Nitric Oxide. Part B, Physiological and Pathological Processes*; Academic Press: San Diego, CA, 1996; Vol. 269.
(8) Nagano, T.; Yoshimura, T. *Chem. Rev.* **2002**, *102*, 1235−1269
(9) Hilderbrand, S. A.; Lim, M. H.; Lippard, S. J. In *Topics in Fluorescence Spectroscopy*; Geddes, C. D., Lakowicz, J. R., Eds.; Springer: 2005; pp 163−188.
(10) Gomes, A.; Fernandes, E.; Lima, J. L. F. C. *J. Fluoresc.* **2006**, *16*, 119−139.

10.1021/ja064955e CCC: $33.50

Scheme 1

(a) Fluorophore displacement by NO

$$\underset{\text{OFF}}{\text{FL}-\text{M}(\text{L}_n)} \overset{\text{NO}}{\rightleftharpoons} \underset{\text{ON}}{\text{FL}} + (\text{L}_n)\text{M}-\text{NO}$$

(b) Copper(II) reduction by NO

$$\underset{\text{OFF}}{\text{FL}-\text{Cu}^{\text{II}}(\text{L}_n)} \xrightarrow[\text{ROH}]{\text{NO}} \underset{\text{ON}}{\text{FL}-\text{Cu}^{\text{I}}(\text{L}_n)} + \text{RONO}$$

(c) Ligand nitrosation via Cu(II) reduction by NO

$$\underset{\text{OFF}}{\text{Cu}^{\text{II}}(\text{FL})} \xrightarrow{\text{NO}} \text{Cu}^{\text{I}} + \underset{\text{ON}}{\text{FL}-\text{NO}}$$

(FL = Fluorophore, M = Metal, L = Ligand)

most available sensors cannot provide direct, real-time imaging of NO. Since NO is relatively stable under physiological conditions,[11] it can be directly monitored. To achieve direct detection of nitric oxide, new sensors are desired that allow for better exploration of NO-induced signaling in biology.

Our laboratory has designed NO sensors employing transition-metal complexes. Interaction of these complexes with NO offers the promise of investigating nitric oxide itself in biological media. In the past few years, we have constructed several metal−fluorophore scaffolds as potential NO sensors, including those based on cobalt,[12−16] copper,[17−19] iron,[15] rhodium,[20] and ruthenium[21] chemistry. Our general strategy for NO sensing is to coordinate a fluorophore ligand to a metal ion to quench the fluorescence, which is restored by the interaction of NO with the metal center, sometimes with release of the fluorophore and concomitant emission turn-on (Scheme 1a).[9] Although all of the metal complexes reported by us can directly interact with NO, most of the metal−fluorophore platforms are either not soluble or are unstable in aqueous solutions. In some cases, water can outcompete the fluorophore for coordination to the metal center.

Recently, we have been exploring Cu(II)-based probes for NO detection. The strategy behind these Cu(II)-based sensors is that formation of a diamagnetic Cu(I) species via NO-triggered reduction alleviates the fluorescence quenching associated with coordination to a paramagnetic Cu(II) center (Scheme 1b).[17,18] Utilizing this strategy, we constructed Cu(II) complexes containing dansyl groups as the fluorophore, which are able to detect NO in pH 9.0 buffered solutions.[17] These Cu(II) dansyl compounds were unable to sense NO at a physiologically more relevant pH, however. Recently, a Cu(II) cyclam complex was reported that demonstrated the potential of Cu(II) systems as

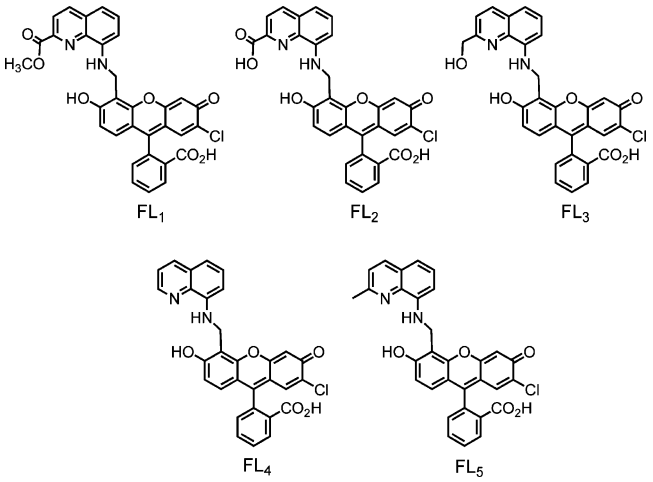

Figure 1. Chemical structures of FL_n ($n = 1-5$).

suitable NO indicators by a strategy different from that used for the Cu(II) dansyl compounds.[22] This complex exhibited fluorescence emission turn-on via NO-induced nitrosation of the fluorophore, which dissociated from the reduced Cu(I) in the buffered methanolic solution (Scheme 1c). Although these various Cu(II)-based systems are not satisfactory as biological NO sensors, the studies formed the basis of a successful approach for developing metal-based sensors to image NO production in live cells.

To achieve NO sensing in a physiological context, five fluorescein derivatives (Figure 1) were prepared for binding Cu(II). These ligands are based on molecules previously described for zinc-sensing bioapplications by our laboratory.[23,24] The copper(II) fluorescein complexes of these ligands react directly with NO, evoking a concomitant emission increase in pH 7.0 buffered solutions. Moreover, the detection of NO by these Cu(II) probes is specific over other reactive nitrogen or oxygen species, including HNO, $ONOO^-$, NO_2^-, NO_3^-, H_2O_2, O_2^-, and ClO^-. The synthesis, NO-sensing ability, and mechanism of fluorescence turn-on of the copper−fluorescein complexes are described in the present work. Density functional theory (DFT) calculations are also presented that address the mechanism of fluorescence turn-on. The imaging of NO production in macrophage and neuroblastoma cells by Cu(FL_5) has recently been described elsewhere.[19]

Experimental Section

Materials and Procedures. All chemical reagents and solvents were obtained from commercial suppliers and used as received. Whatman F254 silica gel-60 plates of 1 mm thickness were used for preparative TLC. Nitric oxide (NO) (Matheson, 99%) was purified by a previously reported method.[20] NO was transferred to the reaction solutions by a gastight syringe in an anaerobic chamber. Fluorescence emission spectra were recorded on a Photon Technology International fluorescence spectrophotometer at 25 or 37 °C. A Varian 300 or 500 NMR spectrometer was used to record ^{1}H and ^{13}C NMR spectra. IR spectra were measured on an Avatar 360 FTIR instrument. UV−vis spectra were obtained on a Hewlett-Packard 8453 diode-array or a Cary 1E

(11) Wink, D. A.; Grisham, M. B.; Mitchell, J. B.; Ford, P. C. *Methods Enzymol.* **1996**, *268*, 12−31.
(12) Franz, K. J.; Singh, N.; Spingler, B.; Lippard, S. J. *Inorg. Chem.* **2000**, *39*, 4081−4092.
(13) Franz, K. J.; Singh, N.; Lippard, S. J. *Angew. Chem., Int. Ed.* **2000**, *39*, 2120−22.
(14) Hilderbrand, S. A.; Lippard, S. J. *Inorg. Chem.* **2004**, *43*, 4674−4682.
(15) Hilderbrand, S. A.; Lippard, S. J. *Inorg. Chem.* **2004**, *43*, 5294−5301.
(16) Lim, M. H.; Kuang, C.; Lippard, S. J. *ChemBioChem* **2006**, web release date June 21, 2006; DOI: 10.1002/cbic.200600042.
(17) Lim, M. H.; Lippard, S. J. *J. Am. Chem. Soc.* **2005**, *127*, 12170−12171.
(18) Smith, R. C.; Tennyson, A. G.; Lim, M. H.; Lippard, S. J. *Org. Lett.* **2005**, *7*, 3573−3575.
(19) Lim, M. H.; Xu, D.; Lippard, S. J. *Nat. Chem. Biol.* **2006**, *2*, 375−380.
(20) Hilderbrand, S. A.; Lim, M. H.; Lippard, S. J. *J. Am. Chem. Soc.* **2004**, *126*, 4972−4978.
(21) Lim, M. H.; Lippard, S. J. *Inorg. Chem.* **2004**, *43*, 6366−6370.
(22) Tsuge, K.; DeRosa, F.; Lim, M. D.; Ford, P. C. *J. Am. Chem. Soc.* **2004**, *126*, 6564−6565.
(23) Chang, C. J.; Lippard, S. J. In *Neurodegenerative Diseases and Metal Ions: Metal Ions in Life Sciences*; Sigel, A., Sigel, H., Sigel, R. K. O., Eds.; John Wiley & Sons: 2006; Vol. 1, pp 321−370.
(24) Nolan, E. M.; Jaworski, J.; Okamoto, K.-I.; Hayashi, Y.; Sheng, M.; Lippard, S. J. *J. Am. Chem. Soc.* **2005**, *127*, 16812−16823.

spectrophotometer. High-resolution mass spectrometric measurements were performed by staff at the MIT Department of Chemistry Instrumentation Facility (DCIF).

X-ray Crystallographic Studies. Single crystals suitable for data collection were mounted in Infineum V8512 on the tips of glass capillaries and frozen in a −100 °C nitrogen cold stream. Data were collected on a Bruker APEX CCD X-ray diffractometer with Mo Kα radiation (λ = 0.71073 Å) controlled by the SMART software package.[25] The general procedures used for data collection are reported elsewhere.[26] Empirical absorption corrections were calculated with the SADABS program.[27] Structures were solved by direct methods and refined with the SAINTPLUS and SHELXTL software packages.[28,29] All non-hydrogen atoms were refined anisotropically. Hydrogen atoms were assigned idealized positions and each was given a thermal parameter equivalent to 1.2 times the thermal parameter of the atom to which it was attached. All structure solutions were checked for higher symmetry with PLATON.[30] In the structure of $[Cu(modL)_2](BF_4)_2 \cdot 2CH_3OH$, the hydrogen atoms of the lattice CH_3OH molecule were not assigned, since the oxygen atom of a CH_3OH molecule was disordered over two positions with occupancy factors of 0.15 and 0.85, respectively. Four fluorine atoms of one BF_4^- anion were also disordered over two positions with occupancy factors of 0.28 and 0.72, respectively, in the structure of $[Cu_2(modL')_2(CH_3OH)](BF_4)_2 \cdot CH_3OH$. The highest electron density in the final difference Fourier maps for $[Cu_2(modL')_2(CH_3OH)]$ $(BF_4)_2 \cdot CH_3OH$ was 1.368 e/Å^3 in the region of the disordered BF_4^- anion.

Computational Details. All geometries were optimized within the density functional theory[31] framework using Jaguar 6.0[32] at the B3LYP/6-31G** level of theory.[33,34] A standard geometry optimization of a fluorescein skeleton in its deprotonated carboxylate form gives the lactone form. This result arises because the fluorescein lactone is the most stable form in the gas phase. Because the LUMO of the xanthene ring is utilized in forming the lactone ring, the lactone is not the active, fluorescent form of the molecule. To obtain the more relevant, ring-opened fluorescein structure, we carried out a full geometry optimization of its protonated carboxylic acid form. The proton was then removed and the carboxylate portion of the molecule reoptimized, keeping the xanthene fragment frozen. Whereas this procedure is an approximate solution to the intrinsic problem of lactone formation, being unavoidable in a gas phase geometry optimization, it is expected to give a qualitatively correct model of the solution-phase geometry of fluorescein. A second problem that needed to be addressed is that both FL_5 and FL_5−NO are dianions at neutral pH, which gives rise to a number of positive orbital energies in gas phase simulations and complicates the interpretation of the computed orbital energies. In previous work, we showed that the perturbative addition of the continuum solvation potential in self-consistent-field calculations leads to physically more meaningful Kohn−Sham wave functions for anionic species.[35,36] We also considered the use of a more elaborate basis set, such as cc-pVTZ-(-f)++ including diffuse functions,[37] which are more appropriate for anions in general, but found the corrections to be unimportant for the aims of this study. We utilize the 6-31G** geometries for simplicity. All orbital energies discussed in this work were computed with the Amsterdam Density Functional (ADF) 2005.01 software package,[38] using a triple-ζ quality basis (TZP), the BLYP functional,[34,39] and the COSMO solvation model[40,41] with ϵ = 78.4.

Syntheses. Precursors of FL_1 and FL_2 were prepared by modification of a previously reported method.[42] The syntheses of 2-[2-chloro-6-hydroxy-5-(quinolin-8-ylaminomethyl)-3-oxo-3*H*-xanthen-9-yl]benzoic acid (FL_4 = QZ1), 2-{2-chloro-6-hydroxy-5-[(2-methylquinolin-8-ylamino)methyl]-3-oxo-3*H*-xanthen-9-yl}benzoic acid (FL_5), and 2-{2-chloro-6-hydroxy-5-[((2-methylquinolin-8-yl)(nitroso)amino)methyl]-3-oxo-3*H*-xanthen-9-yl}benzoic acid (FL_5−NO) were described previously.[19,24]

8-Nitro-2-quinolinecarboxylic Acid Methyl Ester (1). To a solution (20 mL of CH_3OH and 50 mL of Et_2O) of 8-nitro-2-quinolinecarboxylic acid (1.0 g, 4.3 mmol) was added Me_3SiCHN_2 (15 mL, 30 mmol, 2.0 M in Et_2O) until the color of the solution became light yellow. The reaction solution was stirred for 4 h at room temperature. Removal of the solvent provided a light brown solid. The product (0.47 g, 2.0 mmol, 47%) was purified by column chromatography (SiO_2, 1:1 hexanes/EtOAc R_f = 0.55 by TLC). ^{1}H NMR (500 MHz, CD_2Cl_2): δ (ppm) 4.05 (3H, s), 7.74 (1H, t, J = 7.5), 8.11−8.15 (2H, m), 8.31 (1H, d, J = 8.5), 8.43 (1H, d, J = 8.0). HRMS (*m*/*z*): $[M + Na]^+$ calcd for $C_{11}H_8N_2NaO_4$ 255.0382, found 255.0374.

8-Amino-2-quinolinecarboxylic Acid Methyl Ester (2). Ethyl acetate (20 mL) was added to a mixture of **1** (0.18 g, 0.76 mmol) and 10% Pd/C (63 mg), and the solution was deoxygenated by purging with Ar for 20 min. One atmosphere of H_2(g) was introduced to the deoxygenated solution overnight. The solid residues were removed by filtration over Celite. Concentration of the filtrate produced the desired product (0.13 g, 0.66 mmol, 86%). ^{1}H NMR (500 MHz, $CDCl_3$): δ (ppm) 4.05 (3H, s), 6.97 (1H, dd, J = 7.5, J = 1.5), 7.18 (1H, dd, J = 8.3, J = 0.5), 7.44 (1H, t, J = 8.0), 8.13 (1H, d, J = 8.5), 8.19 (1H, d, J = 8.5). HRMS (*m*/*z*): $[M + Na]^+$ calcd for $C_{11}H_{10}N_2NaO_2$ 225.0640, found 225.0638.

(8-Amino-2-quinolinyl)methanol (3). To an ethanol (8 mL) solution of $NaBH_4$ (0.19 g, 4.9 mmol) at 0 °C was added dropwise a THF solution (8 mL) of **2** (0.10 g, 0.50 mmol) over 5 min. The solution was allowed to warm to room temperature with stirring overnight. A saturated aqueous $NaHCO_3$ solution (3 mL) and water (2 mL) were added to the reaction, and the solution was extracted with $CHCl_3$ three times. The collected $CHCl_3$ layer was washed with brine and water and dried with $MgSO_4$. Removal of the solvent provided the desired product (63 mg, 0.36 mmol, 73%). ^{1}H NMR (500 MHz, $CDCl_3$): δ (ppm) 4.95 (2H, s), 7.00 (1H, dd, J = 7.5, J = 1.5), 7.20 (1H, dd, J = 8.0, J = 1.0), 7.29 (1H, d, J = 8.5), 7.36 (1H, t, J = 7.5), 8.12 (1H, d, J = 8.5). HRMS (*m*/*z*): $[M + Na]^+$ calcd for $C_{10}H_{10}N_2NaO$ 197.0691, found 197.0676.

2-{2-Chloro-6-hydroxy-5-[(2-(methylcarboxy)quinolin-8-ylamino)methyl]-3-oxo-3*H*-xanthen-9-yl}benzoic Acid (FL_1). An ethyl acetate (3 mL) solution of **2** (15 mg, 76 μmol) and 7′-chloro-4′-fluoresceincarboxaldehyde[43] (30 mg, 76 μmol) was stirred overnight at room temperature. The resulting red residue was collected, dried in vacuo, and dissolved in dichloroethane (2 mL). To this solution was added $NaB(OAc)_3H$ (19 mg, 0.15 mmol) and the reaction solution was stirred overnight at room temperature. A portion of the crude material was purified by preparative TLC on reverse phase silica gel (R_f = 0.32,

(25) *SMART: Software for the CCD Detector System*, version 5.626; Bruker AXS: Madison, WI, 2000.
(26) Kuzelka, J.; Mukhopadhyay, S.; Spingler, B.; Lippard, S. J. *Inorg. Chem.* **2004**, *43*, 1751−1761.
(27) Sheldrick, G. M. *SADABS: Area-Detector Absorption Correction*, University of Göttingen: Göttingen, Germany, 1996.
(28) *SAINTPLUS: Software for the CCD Detector System*, version 5.01; Bruker AXS: Madison, WI, 1998.
(29) *SHELXTL: Program Library for Structure Solution and Molecular Graphics*, version 6.1; Bruker AXS: Madison, WI, 2001.
(30) Spek, A. L. *PLATON, A Multipurpose Crystallographic Tool*, Utrecht University: Utrecht, The Netherlands, 2000.
(31) Parr, R. G.; Yang, W. *Density Functional Theory of Atoms and Molecules*, Oxford University Press: New York, 1989.
(32) *Jaguar 6.0*; Schrödinger, Inc.: Portland, Oregon, 2003.
(33) Becke, A. D. *J. Chem. Phys.* **1993**, *98*, 5648−5652.
(34) Lee, C. T.; Yang, W.; Parr, R. G. *Phys. Rev. B* **1988**, *37*, 785−789.
(35) Baik, M.-H.; Friesner, R. A. *J. Phys. Chem. A* **2002**, *106*, 7407−7415.
(36) Baik, M.-H.; Schauer, C. K.; Ziegler, T. *J. Am. Chem. Soc.* **2002**, *124*, 11167−11181.
(37) Dunning, T. H., Jr. *J. Chem. Phys.* **1989**, *90*, 1007−1023.
(38) te Velde, G.; Bickelhaupt, F. M.; Baerends, E. J.; Fonseca Guerra, C.; van Gisbergen, S. J. A.; Snijders, J. G.; Ziegler, T. *J. Comput. Chem.* **2001**, *22*, 931−967.
(39) Becke, A. D. *Phys. Rev. A* **1988**, *38*, 3098−3100.
(40) Klamt, A.; Schüürmann, G. *J. Chem. Soc., Perkin Trans. 2* **1993**, 799−805.
(41) Pye, C. C.; Ziegler, T. *Theor. Chem. Acc.* **1999**, *101*, 396−408.
(42) Roth, R.; Erlenmeyer, H. *Helv. Chim. Acta* **1954**, *37*, 1064−1068.
(43) Nolan, E. M.; Burdette, S. C.; Harvey, J. H.; Hilderbrand, S. A.; Lippard, S. J. *Inorg. Chem.* **2004**, *43*, 2624−2635.

CH_3OH/H_2O = 3:0.7) to yield a red solid (16 mg, 27 μmol, 36%). Mp: 155−157 °C (dec). ^{1}H NMR (500 MHz, CD_3OD): δ (ppm) 3.97 (3H, s), 4.79 (2H, s), 6.53 (1H, d, J = 9), 6.61 (1H, s), 6.63 (1H, d, J = 8.5), 6.99 (1H, s), 7.04 (1H, d, J = 8.0), 7.12 (1H, d, J = 8.0), 7.19 (1H, d, J = 7.5), 7.46 (1H, t, J = 8.0), 7.68 (1H, t, J = 7.5), 7.73 (1H, t, J = 7.5), 7.99 (2H, t, J = 8.5), 8.15 (1H, d, J = 9.5). FTIR (KBr, cm^{-1}): 3421 (br, m), 2962 (w), 2917 (vw), 2849 (vw), 1759 (m), 1722 (m), 1627 (m), 1610 (m), 1577 (w), 1565 (w), 1519 (m), 1489 (w), 1445 (w), 1427 (m), 1377 (w), 1283 (w), 1263 (s), 1217 (w), 1149 (w), 1100 (m), 1092 (m), 1063 (w), 1027 (m), 873 (w), 803 (s), 769 (w), 701 (w), 617 (vw), 575 (vw), 545 (vw), 469 (vw), 403 (vw). HRMS (*m*/*z*): $[M - H]^-$ calcd for $C_{32}H_{20}ClN_2O_7$ 579.0959, found 579.0963. Anal. Calcd for $C_{32}H_{21}ClN_2O_7$: C, 66.16; H, 3.64; N, 4.82. Found: C, 66.18; H, 3.53; N, 4.98.

2-{2-Chloro-6-hydroxy-5-[(2-carboxyquinolin-8-ylamino)methyl]-3-oxo-3*H*-xanthen-9-yl}benzoic acid (FL_2). Portions of 8-aminoquinoline-2-carboxylic acid (14 mg, 76 μmol) and 7′-chloro-4′-fluoresceincarboxaldehyde[43] (30 mg, 76 μmol) were added to 2 mL of EtOAc and the reaction solution was stirred overnight at room temperature. After removing the solvent, the resulting red residue was collected and dissolved in dichloroethane (2 mL) followed by the addition of $NaB(OAc)_3H$ (19 mg, 0.15 mmol). The reaction solution was stirred and the solvent was removed after 1 d. The crude product was twice purified by preparative TLC on silica gel (first purification, R_f = 0.11, 5:1 CH_3OH/CH_2Cl_2; second purification, R_f = 0.61, 6:1 CH_3OH/0.1 M HCl), affording a red solid (9.7 mg, 17 μmol, 23%). Mp: 240−242 °C (dec). ^{1}H NMR (300 MHz, CD_3OD/CD_2Cl_2): δ (ppm) 4.72 (2H, s), 6.57 (1H, d, J = 8.1), 6.68 (1H, s), 6.93 (0.5H, d, J = 7.5), 7.00−7.13 (3H, m), 7.20 (1H, d, J = 6.3), 7.32 (0.5H, t, J = 7.5), 7.48 (1H, t, J = 8.1), 7.53−7.61 (2H, m), 8.03−8.14 (3H, m). FTIR (KBr, cm^{-1}): 3404 (br, m), 3048 (vw), 2962 (w), 2923 (w), 2845 (w), 1635 (m), 1609 (m), 1576 (s), 1512 (w), 1459 (m), 1340 (w), 1303 (w), 1261 (m), 1221 (w), 1148 (s), 1094 (s), 1015 (s), 938 (vw), 878 (vw), 859 (vw), 821 (m), 796 (s), 745 (vw), 713 (vw), 690 (vw), 661 (vw), 628 (w), 599 (w), 582 (vw), 550 (w), 527 (vw), 516 (vw), 492 (w), 472 (m), 460 (w), 442 (w), 435 (w), 422 (w), 413 (w), 405 (w). HRMS (*m*/*z*): $[M + Na]^+$ calcd for $NaC_{31}H_{19}ClN_2O_7$ 589.0779, found 589.0786. Anal. Calcd for $C_{31}H_{19}ClN_2O_7$: C, 65.67; H, 3.38; N, 4.94. Found: C, 65.58; H, 3.32; N, 4.79.

2-{2-Chloro-6-hydroxy-5-[(2-hydroxymethylquinolin-8-ylamino)-methyl]-3-oxo-3*H*-xanthen-9-yl}benzoic Acid (FL_3). A solution (EtOAc, 3 mL) of **3** (33 mg, 0.19 mmol) and 7′-chloro-4′-fluoresceincarboxaldehyde[43] (75 mg, 0.19 mmol) was stirred overnight at room temperature. The resulting red residue was collected, dried in vacuo, and dissolved in dichloroethane (2 mL). To the dichloroethane solution was added a portion of $NaB(OAc)_3H$ (48 mg, 0.23 mmol). The solution was stirred overnight and purified by preparative silica TLC (R_f = 0.22, 1:1:0.9 EtOAc/Hx/CH_3OH), affording a red solid (23 mg, 42 μmol, 22%). Mp: 230−231 °C (dec). ^{1}H NMR (500 MHz, CD_3OD): δ (ppm) 4.74 (2H, s), 4.77 (2H, s), 6.53 (1H, d, J = 9.5), 6.73 (1H, s), 6.97−7.00 (2H, m), 7.09−7.17 (3H, m), 7.32 (1H, t, J = 8.0), 7.45 (1H, d, J = 8.0), 7.49−7.56 (2H, m), 7.99 (1H, d, J = 9.0), 8.05 (1H, d, J = 10.5). FTIR (KBr, cm^{-1}): 3427 (br, m), 3059 (vw), 2996 (vw), 2963 (w), 2932 (vw), 2900 (vw), 1634 (vw), 1575 (s), 1519 (w), 1457 (m), 1419 (w), 1376 (m), 1342 (w), 1305 (vw), 1263 (m), 1223 (w), 1151 (w), 1092 (w), 1039 (vw), 925 (vw), 881 (vw), 822 (m), 806 (m), 712 (vw), 649 (vw), 619 (vw), 600 (vw), 550 (vw), 469 (vw). HRMS (*m*/*z*): $[M - H]^-$ calcd for $C_{31}H_{20}ClN_2O_6$ 551.1010, found 551.1003.

$[Cu_2(modL')_2(CH_3OH)](BF_4)_2\cdot CH_3OH$ and $[Cu(modL)_2](BF_4)_2\cdot 2CH_3OH$. Two kinds of crystals were grown by vapor diffusion of Et_2O into a methanol solution (3 mL) of 2-[(quinolin-8-ylamino)methyl]-phenol (modL) (10 mg, 40 μmol) and copper(II) tetrafluoroborate (9.5 mg, 40 μmol) at room temperature overnight. Violet {major product, $[Cu(modL)_2](BF_4)_2\cdot 2CH_3OH$} and green {minor product, $[Cu_2(modL')_2(CH_3OH)](BF_4)_2\cdot CH_3OH$, modL′ = 2-[(quinolin-8-ylamino)methyl]-phenolate} crystals were manually separated for characterization.

Scheme 2 [a]

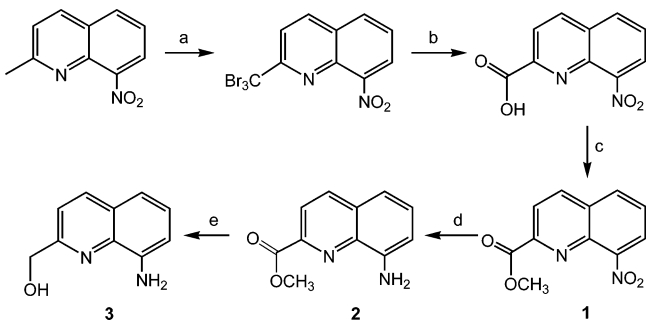

[a] Reagents: (a) Br_2, AcONa, and AcOH (ref 42); (b) 20% H_2SO_4(aq) (ref 42); (c) Me_3SiCHN_2; (d) Pd/C, H_2; and (e) $NaBH_4$.

Quantities of $[Cu_2(modL')_2(CH_3OH)](BF_4)_2\cdot CH_3OH$ sufficient for full characterization were not obtained. FTIR (KBr, cm^{-1}): 3485 (br, w), 3216 (m), 3071 (vw), 2952 (vw), 2931 (vw), 2849 (vw), 1617 (vw), 1598 (vw), 1570 (vw), 1513 (m), 1485 (m), 1454 (m), 1384 (m), 1322 (w), 1265 (s), 1199 (vw), 1130 (sh, w), 1081 (br, vs), 1042 (br, vs), 936 (sh, vw), 903 (vw), 881 (w), 859 (vw), 834 (w), 804 (w), 764 (s), 730 (w), 656 (vw), 633 (vw), 618 (vw), 598 (vw), 581 (vw), 551 (w), 519 (w), 504 (w), 463 (w), 415 (w). Characterization of $[Cu(modL)_2](BF_4)_2\cdot 2CH_3OH$. Mp: 223−225 °C (dec). FTIR (KBr, cm^{-1}): 3379 (br, m), 3246 (m), 3119 (vw), 3070 (w), 3056 (w), 3026 (vw), 2940 (vw), 2864 (vw), 1616 (w), 1596 (m), 1516 (s), 1479 (w), 1462 (s), 1400 (w), 1382 (w), 1358 (w), 1332 (w), 1316 (vw), 1270 (w), 1248 (w), 1188 (w), 1175 (w), 1162 (sh, w), 1133 (sh, w), 1100 (br, vs), 1080 (br, vs), 1039 (sh, vw), 936 (sh, vw), 885 (w), 867 (w), 848 (w), 832 (m), 794 (w), 763 (s), 731 (w), 721 (w), 664 (vw), 559 (vw), 519 (w), 491 (vw). Anal. Calcd for $CuC_{32}H_{28}B_2F_8N_4O_2\cdot 2CH_3OH$: C, 50.93; H, 4.53; N, 6.99. Found: C, 50.41; H, 4.18; N, 6.98.

Results and Discussion

Design Considerations for Cu(II)-Based NO Sensors. Of the various metal-based fluorescent sensors for nitric oxide prepared and evaluated in our laboratory, Cu(II) systems proved to have the greatest potential for application in a physiologically relevant setting.[17−19] Fluorescein-based ligands for Cu(II) were chosen, since fluorescein is water-soluble and highly emissive (Φ = 0.95) and has excitation and emission wavelengths in the visible region,[44,45] which minimizes harm to cellular components during NO imaging. Incorporation of copper-binding units to the fluorescein moiety was achieved in a manner analogous to the synthesis in our laboratory of fluorescent sensors for Zn(II).[23] The target ligands are displayed in Figure 1, FL_4 being the same as QZ1 described previously.[24]

Synthesis of Fluorescein-Based Ligands (FL_n). The general assembly of fluorescein-based sensors with one metal ion binding site containing two nitrogen and one or more oxygen donor atoms (N_2O_n, n = 1 or 2) has been previously achieved in our laboratory by using 7′-chloro-4′-fluoresceincarboxaldehyde.[43] This general synthesis was adopted to prepare copper(II)-based NO sensors in the present study.

The synthesis of amine ligands **2** and **3** was accomplished by modification of a previously reported method, as shown in Scheme 2.[42] 8-Nitro-2-quinolinecarboxylic acid was generated by bromination of 8-nitroquinaldine followed by hydrolysis as described.[42] To prepare 8-nitro-2-quinolinecarboxylic acid methyl ester (**1**), trimethylsilyldiazomethane (Me_3SiCHN_2),

(44) Sjöback, R.; Nygren, J.; Kubista, M. *Spectrochim. Acta Part A* **1995**, *51*, L7-L21.
(45) Brannon, J. H.; Madge, D. *J. Phys. Chem.* **1978**, *82*, 705−709.

Scheme 3

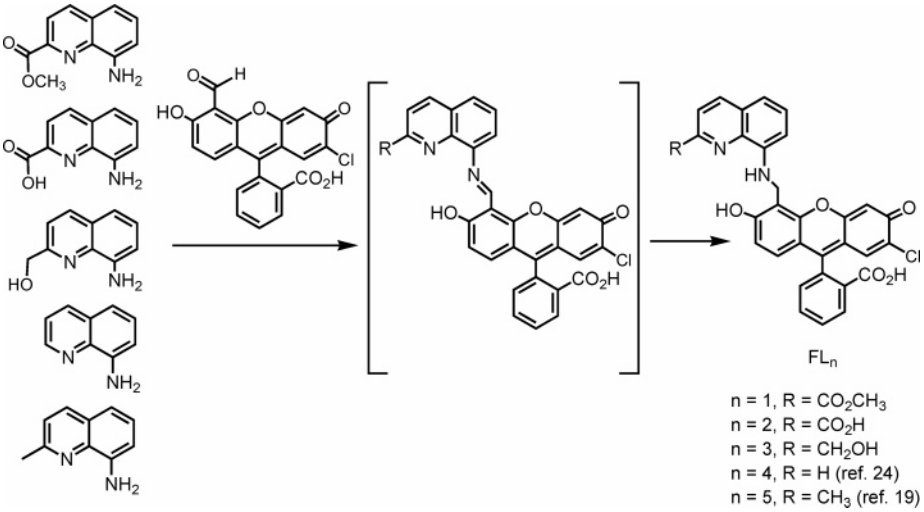

Table 1. Spectroscopic Results[a]

	absorption λ_{max} (nm), ϵ ($\times 10^4$ M^{-1} cm^{-1})		emission λ_{max} (nm), Φ^b or %		
	unbound	Cu(II)[c]	unbound (Φ)	Cu(II)[d] (%)	ref
FL_1	504, 4.3 ± 0.1	499, 4.0 ± 0.1	520, 0.083 ± 0.004	520, 32 ± 2	this work
FL_2	503, 3.8 ± 0.5	496, 3.8 ± 0.3	520, 0.084 ± 0.002	520, 26 ± 3	this work
FL_3	503, 3.9 ± 0.1	497, 3.9 ± 0.5	520, 0.31 ± 0.01	520, 19 ± 2	this work
FL_4	505, 6.9 ± 0.1	496, 5.7 ± 0.1	520, 0.024 ± 0.001	520, 30 ± 3	24 and this work
FL_5	504, 4.2 ± 0.1	499, 4.0 ± 0.1	520, 0.077 ± 0.002	520, 18 ± 3	19 and this work

[a] All spectroscopic measurements were performed at pH 7.0 in 50 mM PIPES, 100 mM KCl buffer. [b] Reported quantum yields are based on fluorescein, $\Phi = 0.95$ in 0.1 N NaOH.[45] [c] One equivalent of $CuCl_2$ was added. [d] Percent fluorescence decrease upon addition of 1 equiv of Cu(II) to a pH 7.0 buffered solution (50 mM PIPES, 100 mM KCl) of FL_n (1 μM), relative to that of free FL_n (50 mM PIPES, 100 mM KCl).

which is a safer alternative to the use of diazomethane, was employed in the present work, affording **1** as a light-brown solid in moderate yield (47%) after purification on silica gel (1:1 hexanes/EtOAc). Hydrogenation of **1** in EtOAc using 10% Pd/C gave pure **2** in 86% yield without further manipulation. Upon reduction of **2** with sodium borohydride in a mixture of THF and EtOH, **3** was obtained in 73% yield without purification.

Scheme 3 illustrates the syntheses of the fluorescein-based ligands FL_1−FL_5. Combination of **2** or **3** (Scheme 2) with 7′-chloro-4′-fluoresceincarboxaldehyde in dry EtOAc resulted in precipitates of the respective intermediate imines, as shown in the scheme. The imines were reduced under mild conditions by using $NaB(OAc)_3H$ in dichloroethane. A portion of the crude materials was purified by preparative TLC, affording desired products FL_1 and FL_3, respectively, in moderate yield. Commercially available amine moieties were assembled with 7′-chloro-4′-fluoresceincarboxaldehyde to obtain pure FL_2, FL_4,[24] and FL_5[19] by a similar procedure. The spectroscopic properties of the FL_n ($n = 1-5$) compounds are summarized in Table 1.

Preparation and Fluorescence Studies of Copper Fluorescein Compounds. The Cu(II) fluorescein complexes Cu(FL_n) ($n = 1-5$, Figure 1) were generated in situ by combining FL_n with $CuCl_2$ in a 1:1 ratio in 50 mM PIPES, pH 7.0, 100 mM KCl buffer. Upon Cu(II) binding to the fluorescein ligands FL_n, a blue-shifted absorption band was observed, compared to that of free FL_n, as summarized in Table 1. UV−visible spectroscopy was employed to verify the binding stoichiometry of the FL_n:Cu(II) complexes at pH 7.0. For FL_1, FL_3, and FL_5,[19] Job's plots of $CuCl_2$:ligand mixtures revealed a break at 0.5, suggesting the formation of 1:1 complexes (Figure 2). For the reactions of FL_2 or FL_4 with $CuCl_2$, however, breaks occurred at values between 0.33 and 0.5, which may indicate the generation of a mixture of 1:1 and 1:2 complexes in pH 7.0 buffered solution. This mixed binding mode of FL_4 with Cu(II) was also observed in the reaction of $Cu(BF_4)_2$ with 2-[(quinolin-8-ylamino)methyl]phenol (modL), investigated as a model for the reaction of FL_4. Two kinds of crystals, $[Cu(modL)_2](BF_4)_2$ and $[Cu_2(modL')_2(CH_3OH)](BF_4)_2$ (modL′ = 2-[(quinolin-8-ylamino)methyl]phenolate), were obtained by vapor diffusion of Et_2O into a methanol solution of $Cu(BF_4)_2$ and modL in a ratio of 1:1 (Figure 3). The observation of 1:1 and 1:2 complexes in the Cu(II) modL system suggests that a similar mixed binding mode for FL_2 and FL_4 with Cu(II) might occur. Also, these crystal structures reveal that one oxygen and two nitrogen atoms of the ligands FL_n might bind to Cu(II), as in the crystal structure of $[Cu_2(modL')_2(CH_3OH)](BF_4)_2$. Crystallographic data for $[Cu(modL)_2](BF_4)_2$ and $[Cu_2(modL')_2(CH_3OH)](BF_4)_2$ are summarized in Tables S2 and S7 (Supporting Information), and selected bond lengths and angles are listed in Table 2.

As shown in Table 1, the fluorescence emission intensities of 1 μM FL_n ($n = 1-5$) pH 7.0 buffered solutions at 37 °C are slightly diminished upon addition of 1 equiv of $CuCl_2$. Introduction of excess NO to buffered Cu(FL_n) (1 μM FL_n and 1 μM $CuCl_2$) solutions (50 mM PIPES, pH 7.0, 100 mM KCl) causes an increase in fluorescence. A 2.5(±0.1)-[46] or 8.3(±0.9)-fold increase in fluorescence was observed in the reaction of Cu(FL_1) or Cu(FL_2) with excess NO over 60 or 70 min (Figure 4a,b). Copper complexes Cu(FL_3) and Cu(FL_4) displayed 3.4(±0.1)-[46] and 31(±1)-fold fluorescence enhancements upon treatment with excess NO over 15 and 20 min, respectively

(46) Preliminary measurements of the reactions of Cu(FL_n) (n = 1, 3) with NO: Tio, J.; Lim, M. H.; Lippard, S. J. *Nucleus* **2006**, *84*, 8−12.

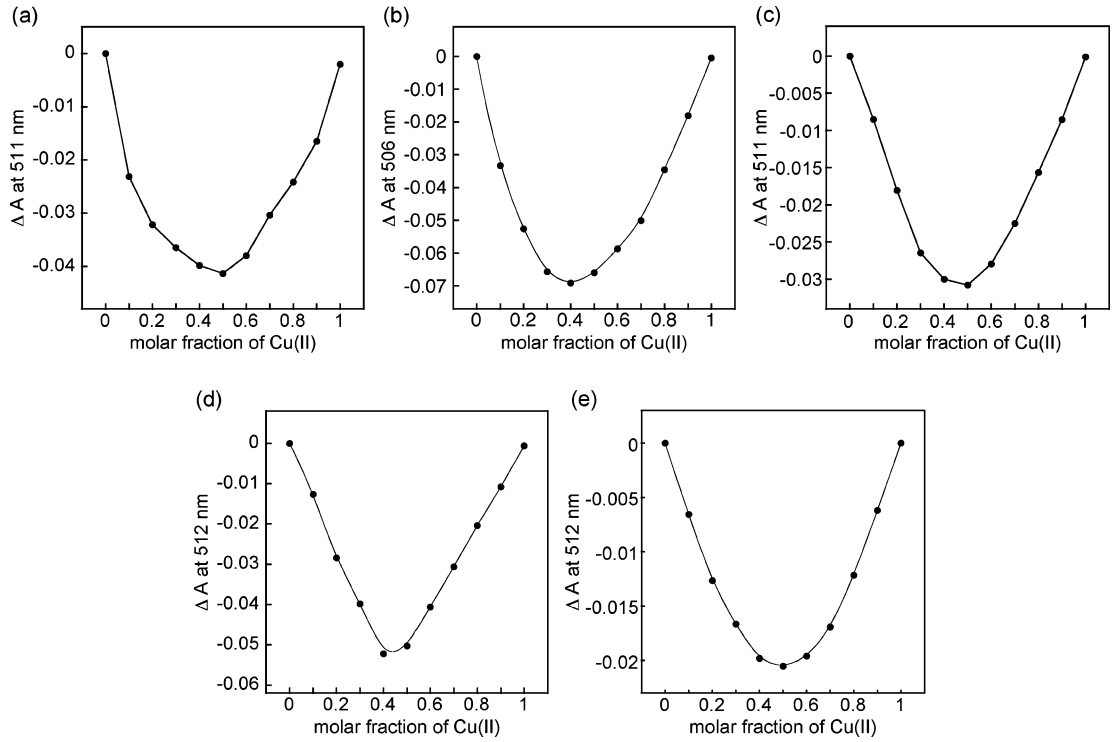

Figure 2. Job's plot for the formation of the FL_n:Cu(II) complex, where $n = 1$ (a), 2 (b), 3 (c), 4 (d), and 5 (e),[19] determined by using UV−vis spectroscopy in a pH 7.0 buffered solution (50 mM PIPES, 100 mM KCl). The concentrations of the initial FL_n ($n = 1-5$) and Cu(II) solutions are 10, 10, 5, 5, and 5 μM, respectively.

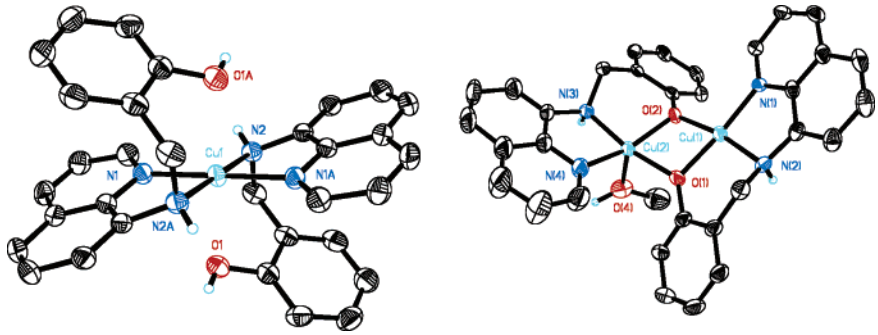

Figure 3. ORTEP diagrams of $[Cu(modL)_2](BF_4)_2$ (left) and $[Cu_2(modL')_2(CH_3OH)](BF_4)_2$ (right) showing 50% probability thermal ellipsoids. The Cu1−O1 distance of 2.492 Å in the structure of $[Cu(modL)_2](BF_4)_2$ indicates a weak interaction. The BF_4^- anions are omitted in the figure.

(Figure 4c,d). Last, a 16(±1)-fold fluorescence increase was observed at 5 min when $Cu(FL_5)$ was allowed to react with excess NO (immediate 11(±2)-fold increase in fluorescence, Figure 4e).[19] The lower limit of $Cu(FL_5)$ for NO detection is 5 nM.[19] The fluorescence response of the $Cu(FL_5)$ probe is specific for NO over other reactive species present in biological systems, including ClO^- (1.9(±0.1)-fold increase), H_2O_2 (1.2(±0.1)-fold increase), NO_3^- (1.2(±0.2)-fold increase), NO_2^- (1.2(±0.2)-fold increase), $ONOO^-$ (2.6(±0.3)-fold increase), and HNO (1.4(±0.2)-fold increase).[19] A 2.0(±0.2)-fold increase in fluorescence was observed when $Cu(FL_5)$ was allowed to react with superoxide ion (O_2^-) that was generated by xanthine and xanthine oxidase (Figure 5).[47,48] Although $Cu(FL_5)$ exhibited a slight fluorescence increase in the presence of peroxynitrite or superoxide ion, it is significantly less than that caused by NO.

Table 2. Selected Bond Lengths (Å) and Angles (deg)[a]

	$[Cu(moL)_2](BF_4)_2 \cdot 2CH_3OH$	$[Cu_2(modL)_2(CH_3OH)](BF_4)_2 \cdot CH_3OH$[b]
Cu1−N1	1.997(2)	1.956(4)
Cu1−N2	2.033(2)	2.009(4)
Cu1−O1		1.928(3)
Cu1−O2		1.947(3)
N1−Cu1−N2	97.24(10)	85.39(17)
N1−Cu1−N2A	82.76(10)	
O1−Cu1−O2		77.47(14)
Cu1−O1−Cu2		100.85(15)
Cu1−O2−Cu2		99.96(15)
N3−Cu2−N4		85.32(18)
O1−Cu2−O2		76.68(14)

[a] Numbers in parentheses are estimated standard deviations in the last significant figures. Atoms are labeled as indicated in Figure 3. [b] Bond lengths and angles of only one of the two crystallographically independent, but chemically identical, molecules are listed.

Fluorescence enhancement in the NO reactions of $Cu(FL_5)$ is not significantly affected in different buffered solutions and

(47) Sono, M. *J. Biol. Chem.* **1989**, *264*, 1616−1622.
(48) Yang, D.; Wang, H.-L.; Sun, Z.-N.; Chung, N.-W.; Shen, J.-G. *J. Am. Chem. Soc.* **2006**, *128*, 6004−6005.

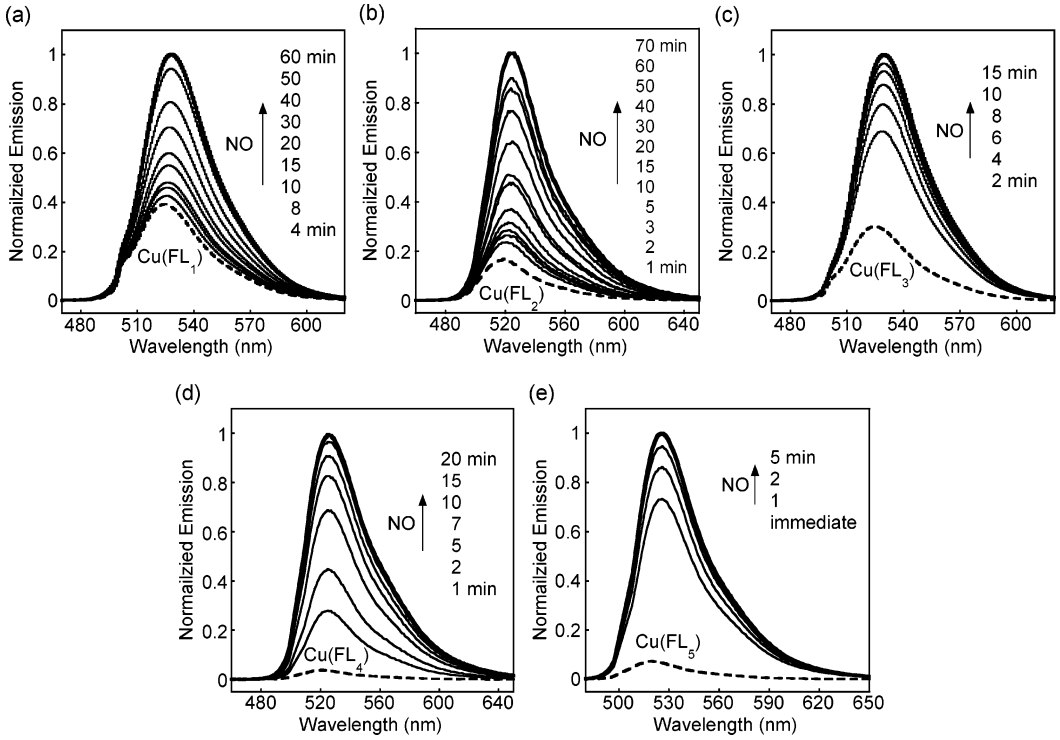

Figure 4. Fluorescence emission spectra of a solution of Cu(FL_n) (1 μM FL_n and 1 μM $CuCl_2$) in deoxygenated buffered solution (50 mM PIPES, pH 7.0, 100 mM KCl) before (dashed line) and after (solid lines) addition of 1300 equiv of NO(g) at 37 °C.

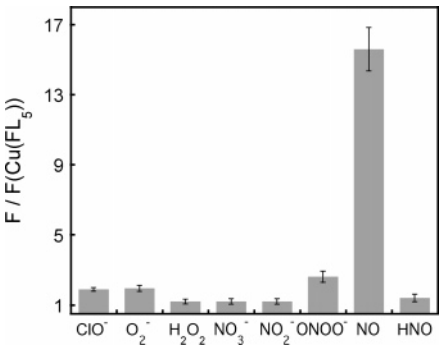

Figure 5. Specificity of Cu(FL_5) for NO at pH 7.0, determined as the fluorescence response of Cu(FL_5) after addition of 100 equiv of ClO^- (sodium hypochlorite), O_2^- (0.1 U xanthine oxidase and 100 μM xanthine), H_2O_2, NO_3^-, NO_2^-, $ONOO^-$ (sodium peroxynitrite), NO (1.9 mM NO-saturated aqueous solution), and HNO (Angeli's salt $Na_2N_2O_3$) for 2 h. The excitation wavelength was 503 nm. All data (F) are normalized with respect to the emission of Cu(FL_5) [F(Cu(FL_5))]. The Cu(II) species Cu(FL_5) was prepared in situ by reacting FL_5 (1 μM) with $CuCl_2$ (1 μM).

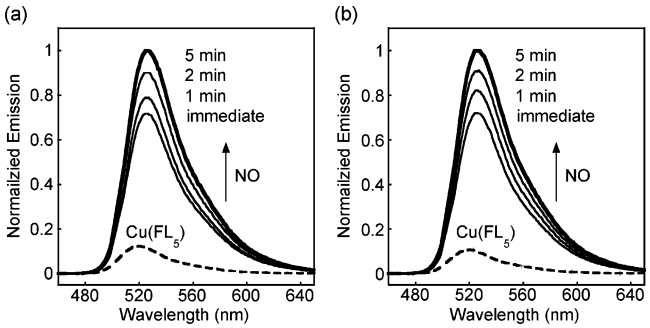

Figure 6. Fluorescence emission spectra of a solution of Cu(FL_5) upon addition of excess NO. (a) Fluorescence response of Cu(FL_5) (1 μM FL_5 and 1 μM $CuCl_2$) in a deoxygenated pH 7.0 buffered solution (20 mM phosphate) before (dashed line) and after (solid lines) addition of 1300 equiv of NO(g) at 37 °C. (b) Fluorescence emission spectra of an aerobic solution of Cu(FL_5) (1 μM FL_5 and 1 μM Cu(NO_3)$_2$) upon admission of 1300 equiv of NO at 37 °C (50 mM PIPES, pH 7.0, 100 mM KNO_3).

is independent of Cl^- ion. When 20 mM potassium phosphate buffer was used to follow the NO reaction of Cu(FL_5), a 10(±2)-fold fluorescence increase occurred over 5 min (Figure 6a). When Cu(FL_5) was prepared in situ by the reaction of Cu(NO_3)$_2$ with FL_5 in a 1:1 ratio, a 12(±2)-fold increase was observed upon addition of excess NO over 5 min (50 mM PIPES, pH 7.0, 100 mM KNO_3), as shown in Figure 6b.

These results demonstrate that Cu(FL_n) can directly detect NO with significant emission turn-on at a physiologically relevant pH. A comparison of the NO reactions of Cu(FL_n) with those of a commercially available NO probe DAF-2 (*o*-diaminofluorescein) clearly highlights the unique ability of copper-based sensors for direct NO sensing. DAF-2 displayed no increase in fluorescence upon addition of excess NO for 1 h in the absence of O_2, but it did exhibit immediate fluorescence turn-on under aerobic conditions, indicating that it is an indirect NO sensor.[19]

Mechanism of Fluorescence Detection of NO by Cu(FL_n). When FL_1 or FL_5 was titrated with $CuCl_2$ at 25 °C, the optical absorption spectral changes could be fit to a one-step binding equation, affording a dissociation constant (K_d) of 0.25(±0.14) or 1.5(±0.3) μM[19] for Cu(II) ion (Figure 7). These K_d values indicate that the reaction solution of FL_1 or FL_5 (1 μM) with $CuCl_2$ (1 μM) contains Cu(II) ion, free FL_n, and Cu(FL_n), as described in Scheme 4. The 6-fold increase in binding affinity of FL_1 compared to FL_5 is consistent with the presence of an additional oxygen atom for copper coordination. To identify the species responsible for NO detection, the fluorescence of a Cu(II)-free FL_5 solution was monitored during treatment with excess NO. There was none of the fluorescence enhancement that was observed in the reaction of Cu(FL_5) with NO.[19] Moreover, no fluorescence increase was observed upon addition

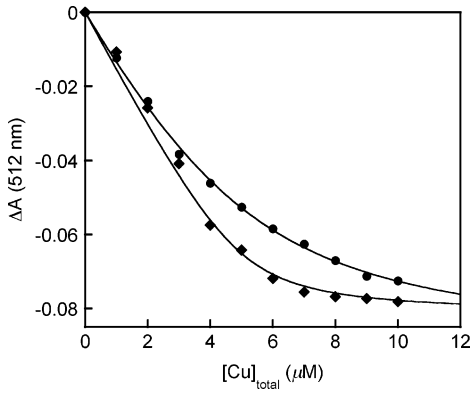

Figure 7. Measurement of the dissociation constant (K_d) of $Cu(FL_1)$ (◆) or $Cu(FL_5)$[19] (●). $CuCl_2$ was titrated into a 5 μM FL_1 or FL_5 solution (50 mM PIPES, pH 7.0, 100 mM KCl). The formation of $Cu(FL_1)$ or $Cu(FL_5)$ was followed by the absorbance change (ΔA) at 512 nm. The titration trace was fit to the equation described previously.[19]

Scheme 4

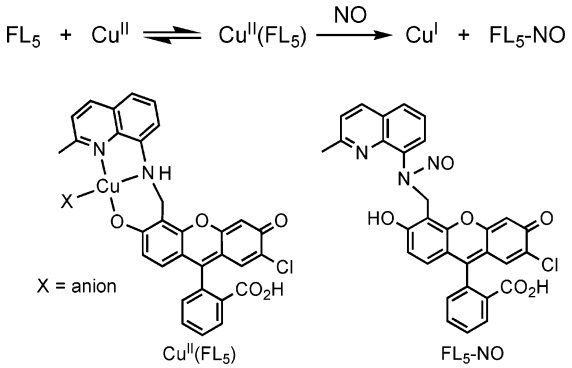

of excess NO to a $Cu(FL_5)$ solution containing the Cu(II) chelator *N*,*N*′-1,2-ethanediylbis(*N*-(carboxymethyl)glycine)-(EDTA).[19] These observations demonstrate that $Cu(FL_5)$, and not FL_5 or Cu(II) ion alone, is the nitric oxide indicator with fluorescence turn-on.

The mechanism of turn-on emission of $Cu(FL_5)$ by NO requires NO-induced reduction of Cu(II) to Cu(I), forming NO^+. Loss of Cu(II) was monitored by EPR spectroscopy.[19] Formation of a diamagnetic Cu(I) complex during NO reactions of Cu(II) complexes can restore the quenched fluorescence of a fluorophore coordinated to the paramagnetic metal.[17,18,22] The fluorescence of FL_5 is unchanged in the presence of $[Cu(CH_3CN)_4](BF_4)$, however.[19] This result indicates that reduction of the copper center from Cu(II) to Cu(I) by NO alone does not cause fluorescence enhancement in the NO reaction of the $Cu(FL_5)$ complex, which differs from prior observations for Cu(II)-based systems.[17,18]

Examination of the reaction of $Cu(FL_5)$ with NO by UV−vis spectroscopy and liquid chromatography−mass spectrometry (LC−MS) revealed that the FL_5 ligand becomes nitrosated to generate FL_5−NO, which dissociates from the copper center.[19] The FL_5−NO species is stable in pH 7.0 buffered solution for several days, as monitored by LC−MS, indicating the irreversible nature of NO sensing by $Cu(FL_5)$. To characterize further the nitrosated product from the reaction of $Cu(FL_5)$ with NO, we independently prepared FL_5−NO.[49] Treatment of a CH_3OH solution of FL_5 containing excess $NaNO_2$(aq) over ice with HCl(aq) immediately induced a color change from red-orange to bright yellow. A precipitate immediately appeared and the supernatant was collected after 30 min by centrifugation. Dialysis of the supernatant against water was performed to remove residual $NaNO_2$. An orange solid was obtained in moderate yield upon lyophilization. The isolated solid analyzed by LC−MS was identical to the material obtained in the reaction of $Cu(FL_5)$ with NO.[19] In addition, the preparation of ^{15}N-labeled nitrosated product FL_5−^{15}NO allowed us to elucidate the site of nitrosation by ^{1}H and ^{15}N NMR spectroscopy. Nitrosation of FL_5 occurs at the secondary amine metal-binding site to create a *N*-nitrosamine, FL_5−NO, as shown in Scheme 4, causing dissociation of nitrosated ligand from the copper center. We next addressed the question of whether FL_5−NO is the species responsible for enhanced emission. The quantum yield of synthetic FL_5−NO was measured to be $\Phi(FL_5\text{−NO}) = 0.58 \pm 0.02$ compared to fluorescein ($\Phi = 0.95$).[45] Thus, FL_5−NO is brighter than FL_5 or $Cu(FL_5)$, for which $\Phi = 0.077 \pm 0.002$ and 0.063 ± 0.002, respectively.[19] These mechanistic studies clearly demonstrate that $Cu(FL_5)$ is capable of fluorescence-based NO sensing at pH 7.0 by NO-induced metal reduction followed by release of the *N*-nitrosated fluorescein ligand from the copper center, triggering concomitant fluorescence enhancement (Scheme 4). The reason for the enhanced emission of the *N*-nitrosated species FL_5−NO, compared to FL_5, was addressed by density functional theory (DFT) calculations (vide infra).

Scheme 5

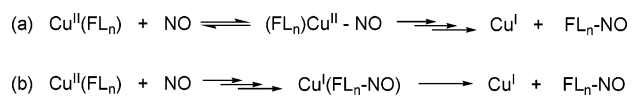

Further elaboration of the reaction pathway shown in Scheme 4 is possible by considering the different observed fluorescence responses of $Cu(FL_n)$ ($n = 1-5$) to NO. Compound FL_5−NO might be formed by several plausible mechanisms. One possibility (Scheme 5a) would involve initial NO coordination to Cu(II) followed by internal electron transfer and migration of NO^+ from the copper(I) center to the amine functionality with loss of a proton to produce the *N*-nitrosamine. A subsequent step would be dissociation of the *N*-nitrosamine from the Cu(I) center. An alternative mechanism of *N*-nitrosamine formation would be direct interaction of NO with the deprotonated amine by an inner sphere electron transfer from the ligand to the copper center to form the *N*-nitrosamine, as described for related chemistry in a recent report (Scheme 5b).[22]

A comparison of the NO reaction rates of the Cu(II) complexes of FL_1, FL_3, and FL_5 reveals that the NO-induced fluorescence increase is slower when FL_n has one additional donor atom coordinated to the Cu(II) center (Figure 1 and Scheme 4). This observation might be explained by one or both of the following possibilities. The Cu(II) complexes containing tetradentate ligands FL_1 or FL_3 may be less able to accommodate the structural rearrangement required for a planar-to-tetrahedral conversion upon Cu(I) complex formation as compared to the tridentate ligand FL_5. As a result, the rates of NO reactions of $Cu(FL_n)$ ($n = 1, 3$), compared with that of $Cu(FL_5)$, are lower, reducing the rate of formation of the FL_n−NO species responsible for fluorescence enhancement. The second possibility concerns the dissociation of FL_n−NO from copper. The presence of an additional donor atom in the FL_n chelate may decelerate

(49) Lee, J.; Chen, L.; West, A. H.; Richter-Addo, G. B. *Chem. Rev.* **2002**, *102*, 1019−1065 and references therein.

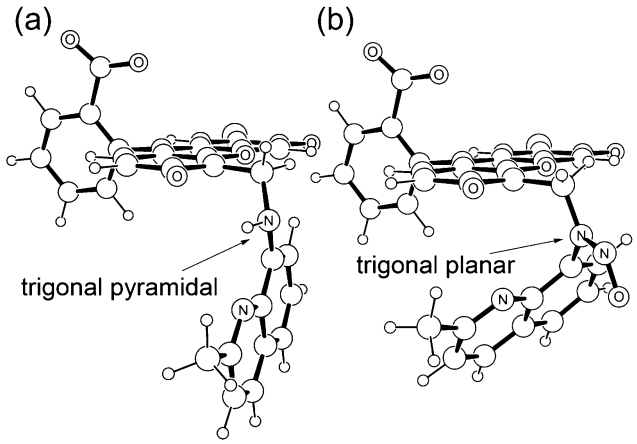

Figure 8. DFT-optimized structures of (a) FL_5 and (b) FL_5−NO.

dissociation of FL_n−NO from copper, which would also result in a slower fluorescence increase. A comparison of the K_d values for Cu(FL_1) and Cu(FL_5), 0.25 ± 0.14 and 1.5 ± 0.3 μM (Figure 7), respectively, supports this notion, assuming that the K_d values for the *N*-nitrosated amine product may follow this trend. At present, we are unable to determine whether one or both of these factors play a significant role in influencing the NO reactivity of Cu(FL_n). More detailed kinetic studies of these and additional complexes are required to establish how the structure and composition of the copper−fluorophore complex affects its NO reactivity.

Introduction of additional donor atoms to FL_n should also affect the electronic properties of the copper center. To address this issue, electrochemical studies were attempted. Measurements of the Cu(FL_n) redox potentials in a mixture of 1:9 DMSO and DMF, however, were unsuccessful, the redox potential of free Cu(II) ion being mainly observed. This result might be a consequence of the micromolar K_d values for the equilibrium in Scheme 4, measured for Cu(FL_n) (n = 1, 5) in aqueous buffer and assuming similar values in the DMSO/DMF mixed solvent, and the corresponding presence of significant concentrations of free Cu(II) ion in solution.

Although the mechanism of the NO reactions with Cu(FL_n) is not unequivocally established by these experiments, the present work suggests that both electronic effects and the equilibrium between bound and free copper will affect formation of the *N*-nitrosamine. Irrespective of the mechanism, however, the ability of the Cu(FL_n) complexes to detect NO described here provides a valuable NO sensing strategy, and improved versions based on this platform should enable the elucidation of NO function in vivo.

Theoretical Analysis of the Relative Fluorescence of FL_5 versus FL_5−NO. The "off−on" properties of fluorescence-based sensors such as FL_n may operate by the well-established photoinduced electron transfer (PET) mechanism.[50−52] In PET, the presence of a covalently bound nitrogen atom with a lone pair of electrons will quench the fluorescence of the sensor in the absence of an analyte. Perturbation of this nitrogen atom lone pair, such as by coordination to a diamagnetic metal ion,[24]

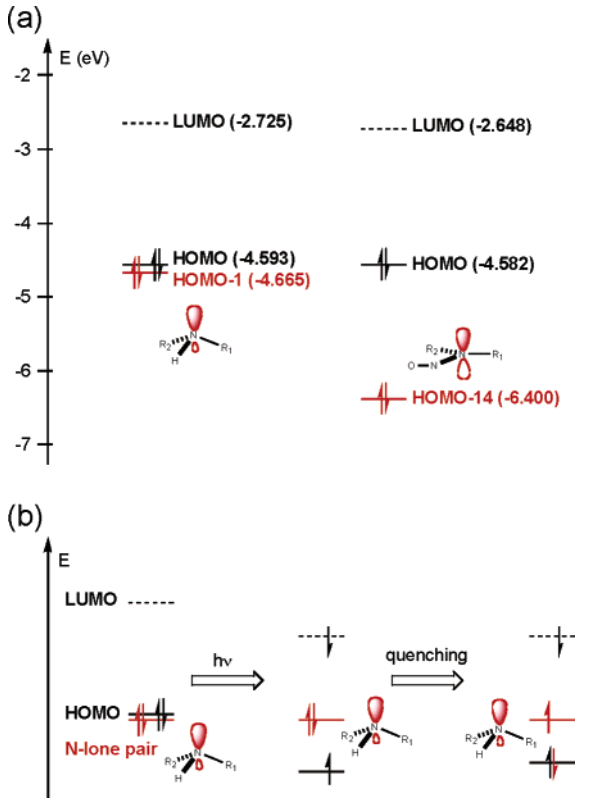

Figure 9. (a) Relative energies of the molecular orbitals for the ground states of FL_5 (left) and FL_5−NO (right). The NNO-based orbital, HOMO-14, of FL_5−NO is expected to be too low in energy to serve as a donor for fluorescence quenching. (b) Qualitative molecular orbital diagram for the ground (left), excited (middle), and charge-transfer (right) states of FL_5. The lowering of the HOMO and LUMO associated with the fluorophore in the excited state is due to electronic relaxation, which would not be expected to alter significantly the energy of the nitrogen-based MO. Nonradiative relaxation of the charge-transfer state returns the molecule to the ground state. R_1 = 2-methylquinoline and R_2 = fluorophore.

will alleviate this quenching process, causing fluorescence "turn-on." Note that binding to a paramagnetic metal ion such as Cu(II) is expected to preserve or enhance the quenching behavior of fluorophores.[53]

For the FL_5/FL_5−NO system, both species have a nitrogen atom-based lone pair of electrons that might be expected to contribute to fluorescence quenching, raising the important question of why fluorescence "turn-on" occurs at all in the nitrosated species. The DFT-computed geometries (Figure 8) illustrate an important structural difference between FL_5 and FL_5−NO. Whereas the amino functionality in FL_5 adopts a trigonal pyramidal geometry, a trigonal planar structure occurs at the lone-pair-carrying N atom in FL_5−NO. This result indicates that the amino functionality becomes rehybridized to a sp^2 center upon nitrosation. The MO diagrams for FL_5 and FL_5−NO given in Figure 9a illustrate the electronic difference between the two lone pair orbitals. The energy of the donor lone pair orbital in FL_5 (HOMO-1) is −4.665 eV, being essentially isoenergetic with the HOMO. In FL_5−NO, however, the analogous donor orbital (HOMO-14) displays an orbital energy of −6.400 eV, 1.82 eV lower in energy than the HOMO. The HOMO and LUMO orbitals of FL_5−NO are largely identical in character and energy with those computed for FL_5.

(50) Chanon, M.; Hawley, M. D.; Fox, M. A. In *Photoinduced Electron Transfer*; Fox, M. A., Chanon, M., Eds.; Elsevier: Amsterdam, 1988; Part A, pp 1−60.
(51) Callan, J. F.; de Silva, A. P.; Magri, D. C. *Tetrahedron* **2005**, *61*, 8551−8588.
(52) Tanaka, K.; Miura, T.; Umezawa, N.; Urano, Y.; Kikuchi, K.; Higuchi, T.; Nagano, T. *J. Am. Chem. Soc.* **2001**, *123*, 2530−2536.
(53) Chang, J. H.; Choi, Y. M.; Shin, Y.-K. *Bull. Kor. Chem. Soc.* **2001**, *22*, 527−530.

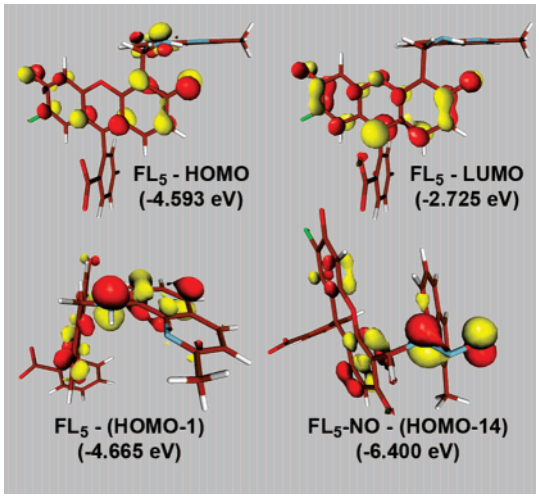

Figure 10. Isosurface plots (isodensity value = 0.5 au) of the key molecular orbitals in the FL_5/FL_5-NO system. The HOMO, LUMO, and HOMO-1 of FL_5 and HOMO-14 of FL_5-NO are illustrated.

These most important orbitals are depicted in Figure 10. For a fluorophore to be quenched by an electron donor group, the MO associated with that donor must lie energetically within the region of the frontier orbitals associated with the fluorophore (Figure 9b), in addition to having the correct orientation to couple effectively with the acceptor orbital, to maximize the electron-transfer efficiency. For FL_5, the nitrogen atom lone pair is conjugated into the quinoline group, where an antibonding π-interaction helps to increase its energy, as can be seen from the node between these two groups [FL_5-(HOMO-1), Figure 10]. Excitation of the fluorophore causes a reordering of these MOs due to electronic relaxation in the excited state, which does not affect the energy of the donor orbital to a significant extent. Electron transfer from the donor orbital into the now lower-lying, half-occupied MO of the fluorophore brings about the observed quenching (Figure 9b).

In the case of FL_5-NO, the donor nitrogen atom has a nearly planar geometry with a normal vector in the plane of the quinoline group [FL_5-NO-(HOMO-14), Figure 10], thus preventing the same out-of-phase π-interaction conjugation present in FL_5. Instead, the nitrogen atom lone pair interacts with the π-system of the formally cationic NO^+ group, producing a stabilized MO at a significantly lower energy. This MO lies well below the frontier orbitals of the fluorophore and cannot serve as an electron donor for the purposes of quenching. Although it is impossible to determine quantitatively the orbital energies of the excited state within the framework of DFT, it is clear that lowering the donor orbital energy in the ground state will translate analogously to the excited state, offering a qualitative rationale for the experimentally observed fluorescence "turn-on" of the *N*-nitrosated species.

Summary and Perspective. Five fluorescein-based ligands (FL_n, $n = 1-5$) were synthesized as a framework for Cu(II)-based complexes that could serve as biosensors for nitric oxide. The Cu(II) species $Cu(FL_n)$ generated in situ by reaction of FL_n with $CuCl_2$ exhibit a significant increase in fluorescence upon addition of NO in pH 7.0 buffered aqueous solution. Turn-on emission of $Cu(FL_5)$ by NO occurs by reduction of Cu(II) to Cu(I), forming NO^+, which nitrosates FL_5 to create FL_5-NO, as revealed by spectroscopic and product analyses of the reaction. Dissociation from the copper center leads to emission turn-on. DFT calculations of FL_5-NO relative to FL_5 also indicate how *N*-nitrosation of FL_5 triggers fluorescence enhancement. The $Cu(FL_n)$ probes facilitate direct NO detection, using metal coordination chemistry with fluorescence enhancement at pH 7.0, when excited at a visible wavelength. The fluorescence response to NO of $Cu(FL_n)$ is specific over other biologically relevant reactive species such as O_2^-, H_2O_2, NO_2^-, NO_3^-, HNO, $ONOO^-$, and ClO^-. Therefore, the Cu(II) fluorescent complexes can directly and specifically detect NO at a physiologically relevant pH.

Although these compounds represent a significant advance, there are some important improvements that need to be addressed in future work. The binding of NO is not reversible, so strictly speaking the molecules are detectors of NO, not true sensors. A reversible sensor for biological NO would be a valuable contribution. Second, the fluorescein construct needs to be modified to allow the molecules to become trapped in cells and not to diffuse out, an important property for imaging live brain slices.[54−56] Finally, it would be useful to have a ratiometric version, in which NO binding causes a change in the fluorescence excitation or emission wavelength, as well as derivatives that can be positioned in a site-specific manner in living tissue.

Acknowledgment. This work was supported by grants from the National Science Foundation (S.J.L.) and the National Institutes of Health (M.-H.B.). The NSF is acknowledged for computational resources (0116050 at IU). M.H.L. thanks the Martin Family Society at MIT for fellowship funding. Spectroscopic instrumentation at the MIT DCIF is maintained with funding from NIH Grant 1S10RR13886-01 and NSF Grants CHE-9808063, DBI9729592, and CHE-9808061. We thank Dr. Rodney P. Feazell for assistance with the X-ray structural work and Dr. Elizabeth M. Nolan for helping with ligand synthesis and providing FL_4 (QZ1).

Supporting Information Available: Cartesian coordinates of computed structures, tables of complete bond distances and angles, and other X-ray crystallographic files (CIF files). This material is available free of charge via the Internet at http://pubs.acs.org.

JA064955E

(54) Tsien, R. Y. *Nature* **1981**, *290*, 527−528.
(55) Tsien, R. Y.; Pozzan, T.; Rink, T. J. *J. Cell Biol.* **1982**, *94*, 325−334.
(56) Woodroofe, C. C.; Masalha, R.; Barnes, K. R.; Frederickson, C. J.; Lippard, S. J. *Chem. Biol.* **2004**, *11*, 1659−1666.